Plant, Cell & Environment

Plant, Cell and Environment (2014) **37**, 2667–2678 doi: 10.1111/pce.12315

Original Article

Water relations of *Robinia pseudoacacia* L.: do vessels cavitate and refill diurnally or are R-shaped curves invalid in *Robinia*?

Ruiqing Wang, Lingling Zhang, Shuoxin Zhang, Jing Cai & Melvin T. Tyree

College of Forestry, Northwest A&F University, Yangling 712100, China

ABSTRACT

Since 2005, an unresolved debate has questioned whether R-shaped vulnerability curves (VCs) might be an artefact of the centrifuge method of measuring VCs. VCs with R-shape show loss of stem conductivity from approximately zero tension, and if true, this suggests that some plants either refill embolized vessels every night or function well with a high percentage of vessels permanently embolized. The R-shaped curves occur more in species with vessels greater than half the length of the segments spun in a centrifuge. Many have hypothesized that the embolism is seeded by agents (bubbles or particles) entering the stem end and travelling towards the axis of rotation in long vessels, causing premature cavitation. VCs were measured on *Robinia pseudoacacia* L. by three different techniques to yield three different VCs; R-shaped: Cavitron P_{50} = 0.30 MPa and S-shaped: air injection P_{50} = 1.48 MPa and bench top dehydration P_{50} = 3.57 MPa. Stem conductivity measured in the Cavitron was unstable and is a function of vessel length when measured repeatedly with constant tension, and this observation is discussed in terms of stability of air bubbles drawn into cut-open vessels during repeated Cavitron measurement of conductivity; hence, R-shaped curves measured in a Cavitron are probably invalid.

Key-words: Cavitron; centrifuge method; exponential curves; vulnerability curve.

INTRODUCTION

Plants transport metastable water (tensile water) under negative pressure (Tyree & Zimmermann 2002). The transport system is vulnerable to embolisms because if an air bubble enters a conduit filled with tensile water, the bubble (or vacuum void) will expand to fill the entire conduit, rendering it incapable of further transport of tensile water until it can be refilled by some mechanism. Transport of tensile water is possible because of the unique structure of xylem conduits, which tend to be numerous for pathway redundancy and separated from each other by pit membranes that prevent passage of air from an embolized to water-filled conduit. Different species have different conduit structures, which confer different vulnerabilities to cavitation events. Smaller vessels tend to be safer than large vessels (Cai & Tyre 2010), but it is the porosity of the pit membranes between adjacent vessels that seems to be of paramount importance because the surface tension of water acting at the pit membrane site prevents bubble propagation between adjacent vessels (Tyree & Zimmermann 2002). A vulnerability curve (VC) is a plot of the percentage loss of hydraulic conductivity (*PLC*) in stems as a function of tension (minus xylem fluid pressure). A large number of articles have revealed two kinds of VCs classified by their shape: R-shaped (or exponential) curves tend to increase in *PLC* from zero tension, whereas S-shaped (or sigmoid) curves tend to be at zero *PLC* for a range of tensions to a critical tension (T_{crit}), beyond which *PLC* increases rapidly to 100% following a sigmoid curve as tension increases.

Plants with S-shaped curves are conservative because their stomata remain partly open, permitting carbon gain and transpiration until xylem tension reaches T_{crit} and then the stomata close to prevent excessive embolism in the stems. In contrast, plants with R-shaped curves suffer substantial *PLC* every day, but keep their stomata open while the stems lose 50–90% of their water conductivity. These plants seem to survive day to day by having a mechanism to refill conduits every night (Cochard *et al*. 2013) or by surviving with only a small percentage of functional vessels. Species that refill diurnally are relatively rare but increasing numbers have been reported [see, e.g. *Vitis* (Brodersen *et al*. 2010), *Acer* and *Fraxinus* (Zwieniecki & Holbrook 1998), *Quercus* (Taneda & Sperry 2008; Sperry *et al*. 2012), *Laurus* (Salleo *et al*. 1996), *Taxus* (Zhang & Richter 1996) and *Robinia* (An *et al*. 2006)].

Recently, Sperry (2013) and Wheeler *et al*. (2013) have questioned the veracity of evidence for refilling in many species. Refilling is usually measured by observing diurnal changes in native *PLC* (*NPLC*), but these measurements are subject to error if stem segments are harvested while still under tension. Cutting stems under tension seems to induce extra embolisms not present before the cutting. Because air bubbles take hours to days to dissolve once tension is relieved (Tyree & Yang 1992; Yang & Tyree 1992), it is recommended that stems be harvested and rehydrated prior to

Correspondence: J. Cai. Fax: +86 029 87080363; e-mail: cjcaijing @163.com; and M. T. Tyree. Fax: +86 029 87080363; e-mail: mel.tyree @cantab.net

excising the stem segments used to measure *NPLC*. Still, any species with an R-shaped curve is a candidate for a species that might cavitate and refill diurnally.

Much debate in the literature has been directed also to the veracity of R-shaped VCs measured by some centrifuge techniques (particularly the Cochard Cavitron). If R-shaped curves are an artefact of measuring technique, then the number of potential candidates for diurnal refilling can be dramatically reduced. In a critical review of methods of measuring VCs, Cochard *et al.* (2013) showed that R-shaped curves are more common in species with long vessels and the percentage of species with R-shaped vessels seems to be a function of the method used to measure VCs. When a Sperry-type centrifuge is used, 85% of long-vessel (ring porous) species appear to have R-shaped curves versus <25% when measured by more traditional methods (bench top dehydration and air injection).

Given the concerns regarding the above methodological techniques of measuring *NPLC* and VCs, all species that have been reported in the past to have R-shaped curves or reported to refill diurnally have to be re-examined. The aims of this article are (1) to re-examine *Robinia pseudoacacia* and (2) to gain further insights into the cause of R-shaped curves in species measured in the Cochard Cavitron. It has been suggested, for example, that R-shaped curves are the result of pre-mature embolism caused in long-vessel species because air bubbles or solid particles can travel to the centre of the axis of rotation in a centrifuge where the highest tension exists, and hence, the bubbles or particles can expand to seed embolisms. In contrast, in short-vessel species, such particles are filtered out by pit membranes and do not induce cavitation near the centre. Our hypothesis is that air bubbles, if present, ought to induce cavitation at a very small tension ($T \leq 0.1$ MPa) because the critical tension for bubble expansion $= 2\tau/r$, where τ is the surface tension of air–water interface and r is the radius of the bubble. An air bubble is 'more vulnerable' than a solid particle because it will expand to fill the entire conduit even before tension exceeds the pressure equivalent of a perfect vacuum (about 0.1 MPa), whereas a solid particle might not seed a cavitation until much larger tensions. Therefore, if you simply spin stems with long vessels at $T \leq 0.1$ MPa long enough, then substantial increases in *PLC* are ought to be observed due to air bubbles.

MATERIALS AND METHODS

Plant material

Experiments were conducted from May to December in 2013 on *R. pseudoacacia* L. trees growing about 5 m above the water level on the bank of the Weihe River in Yangling, Shaanxi, China (34°16′N 108°4′ E, 457 m a.s.l.). Most samples were collected from four trees of 5–7 m tall. All of the measurements were carried out on current-year stems harvested from the southern crown of the trees. For laboratory experiments, shoots of 1.4–2 m long were excised because preliminary air injection experiments indicated that maximum vessel length was <1 m. After spraying leaves with water, branches were enclosed in humidified black plastic bags before excising to retard water loss. The shoots were brought to the laboratory within half an hour after excision and submerged in water for at least 30 min to release the xylem tension.

Length of vessels

Vessel length was measured by the 'air method' as described by Cohen *et al.* (2003), with some modification. Briefly, long shoots were cut with a sharp razor blade and injected with compressed air (0.15 MPa) from the distal side of 6-mm-diameter stems while the basal end was immersed in water. Stem segments (2 cm long) were sequentially excised until bubbling was observed, and the length of remaining stem was recorded as the maximum length of the vessel.

The bubbles flowing out from the basal end were collected in a volumetric cylinder by the water displacement method, and the volume of air was determined when the water surface inside and outside the cylinder were at the same level in order to be sure that the air volume was measured at atmospheric pressure. The gravimetric water displacement method was used to measure air volume since this allowed more precision than reading the scale on the volumetric cylinder. Firstly, the cylinder was filled to the top with water, and then the water was delivered to a balance to measure the maximum water content (W_i). After measuring the air displacement for a measured time interval (ΔT), the cylinder was held at a shallow angle with the open end below the water and the air/water interface at the water level. The end of the cylinder was covered to avoid spilling of water and the cylinder was lifted out of the water. The water remaining in the cylinder was again delivered to a balance and measured (W_f). The air flow rate [Q (mL/min)] was computed from $(W_i - W_f)/(\Delta T\rho)$, where ρ is the density of water displaced by the air.

The air flow rate [Q (mL/min)] was measured at different stem lengths with the air pressure at the inlet and outlet ends being held constant. Under such conditions of constant air pressure drop, the hydraulic conductivity of the cut-open vessels to the air (C) should be proportional to Qx (see eqn 4 in Cohen *et al.* 2003), where x is the stem length at which the air flow rate (Q) was measured. Using the theory of Cohen *et al.* (2003), we assume that

$$C = C_0 \exp(-kx) \text{ or } Qx = Q_0 x_0 \exp(-kx) \quad (1)$$

where C_0 is the limiting conductivity as x approaches zero, k is an extinction coefficient and x is the stem length. A plot of natural log of C versus x resulted in a linear plot, from which k was evaluated from the slope. According to the theory, the most common or mode vessel length (L_{mode}) equals $-1/k$. Mean vessel length was calculated from $L_{mean} = 2L_{mode}$. Similar measurements were carried out on other shoots, with the difference that air was injected from the basal end of the stem segment, and we found no significant difference in the computed mean and mode vessel lengths.

Keeping solutions clean

Our laboratory started doing repeated cycles of embolism and flushing on the same stem and we discovered that extraordinary steps had to be taken to prevent plugging in long stem segments (0.274 m) and to achieve the same K_{max} after each cycle. An ultra-pure water system (model GYJ1-10 L-S; Huachuang Inc., Chongqing, China) was used to make water with particles <10 nm in diameter (guaranteed to produce <1 particle/mL) and the ultra-purer water was used to make 0.1 M KCl solution. Flushing was carried out with degassed KCl solution stored in a stainless steel captive air tank (model 3400-002; SHURflo Inc., Cypress, CA, USA). Even stainless steel rusts a little when in contact with KCl, so to eliminate plugging rust particles, the tank was disassembled and cleaned two to three times per week. Stainless steel surfaces remain shiny because the rust particles easily fall off the surface of stainless steel; other metallic tanks should be avoided. Post-filtering of flushing solution was carried out through an in-line filter (0.3 μm porousity, model 9933-05-AAQ; Parker Hannifin Corp., Rochester, NY, USA). Furthermore, the water in the captive air tank needs to be left unpressurized when not used for flushing; otherwise, air migrates through the rubber bag in sufficient quantity to supersaturate the water with air, which effervesces like flat soda water when depressurized. All of the above steps are necessary for consistent results.

Vulnerability curves

VCs were measured by the Cochard Cavitron technique (Cochard 2002; Cochard *et al*. 2005) using a custom-modified centrifuge. Details about the construction and use of the Cochard Cavitron are described in Cai & Tyree (2010).

Briefly, the Cavitron allows measurement of stem-segment hydraulic conductivity while the stems are spinning in a centrifuge. The maximum conductivity (K_{max}) was measured at a slow spin rate, which causes little or no embolism. Increasing the spin rate increased the tension (T) and the stem conductivity K_h declined. Percentage loss conductivity was computed from

$$PLC = 100(1 - K_h/K_{max}) \quad (2)$$

at each T. VCs were measured on stem segments that are 27.4 cm long, and the typical curve contained 30–50 points of PLC versus T. Each point in the VC was the mean of 5–8 measurements of PLC at any given T and the VCs were fitted to a single Weibull curve (Eqn 3a) or a dual Weibull curve (Eqn 3b) using the software (CavAnal) written by MTT:

$$PLC/100 = 1 - \exp\left[-(T/B)^C\right] \quad (3a)$$

$$PLC/100 = \alpha\left\{1 - \exp\left[-(T/B_1)^{C1}\right]\right\} + (1-\alpha)\left\{1 - \exp\left[-(T/B_2)^{C2}\right]\right\} \quad (3b)$$

where the Weibull constants were obtained by minimizing root mean square error (RMS_{error}). Typical fitted VCs had an RMS_{error} of 2–4%. The value of T at 50% PLC (P_{50}) was then computed from

$$P_{50} = B[\ln(2)]^{1/C} \quad (4)$$

VCs were measured on both flushed and unflushed stems (with native embolism of about 30%). Preliminary experiments revealed that a flush time of 4 min at 150 kPa pressure was adequate to reverse embolism because of the long vessels in our species. In contrast, flush times of 30 min are needed for species with short vessels (6 cm long), based upon other experiments carried out at the same time on a *Populus* clone. VC measurements and flushing were carried out with the ultra-pure water used to make 0.1 mM KCl.

Diurnal variation of native xylem tension

Native xylem tensions (T_{nx}) were measured by the bagged-leaf technique using a portable pressure chamber (model 1515D; PMS Instruments Co., Corvallis, OR, USA). T_{nx} was determined by sealing a leaf in a Ziploc bag covered with aluminium foil bag in order to stop transpiration from the bagged leaf. Leaves remained in the shaded bags >1 h prior to harvest for pressure chamber measurement, at which point the leaves are in equilibrium with T_{nx} in stems. Measurements were conducted on 3 hot and sunny days from 0530 h (pre-dawn) to 2030 h (after the sunset) at 1 h intervals each day. Generally, 6–10 replicate measurements of T_{nx} were performed at each hour. The time of maximum T_{nx} value also was used for the sampling time determination in *NPLC* measurements.

Pre-dawn and midday *NPLC*

This experiment was conducted in May 2013. Pre-dawn samples were collected before sunrise between 0530 and 0600 h on sunny days. Midday samples were collected between 1400 and 1500 h on the same day with the pre-dawn PLC test. PLCs of pre-dawn and midday stems were assessed by low pressure flow meter (LPFM) as described by Tyree *et al*. (1993), with some modification. Shoots were sprayed with water, enclosed in a black plastic bag, excised and then returned to the laboratory within 30 min. Whole shoots were placed under water for at least 30 min to release tension, and then leaves were excised under water to further release tension. These steps were designed to avoid embolism induced by cutting before relaxation of native tension (Wheeler *et al*. 2013). Approximately 2-cm-long stem segments with a diameter about 6.5 mm were excised under water, then mounted on a conductivity system filled with ultra-pure, degassed 0.1 M KCl solution pre-filtered to 10 nm and post-filtered to 0.3 μm. Initial conductivity ($K_h = K_i$) was measured by flowing KCl solution from a reservoir through the segment and onto a computer-interfaced balance with a pressure difference of about 3 kPa. The stems were then flushed with a pressure of 150 kPa for 1 min to remove air bubbles. The hydraulic conductivity was determined again and the flushing was repeated until attaining a maximum

conductivity (K_{max}). *PLC* was calculated from Eqn 2. The tubing and valves of the LPFM were cleaned weekly by filling tubing and valves with Clorox bleach (2%) and allowing it to stand for 24 h (or 4% bleach overnight).

VCs by bench top dehydration

VCs by bench top dehydration (Tyree & Dixon 1986; Sperry *et al*. 1988) were constructed by plotting stem *PLC*s against corresponding xylem tension values measured on bagged leaves. Shoots were sampled in the morning and dehydrated on a bench in the laboratory at room temperature to obtain a series of xylem tensions covering a range of *PLC*s. Dehydration times never exceeded 24 h and usually took less than 6 h. The whole shoot was tightly wrapped in a black plastic bag once the shoot had reached the desired tension. After a minimum of 1 h of equilibration, three leaves were excised from the shoot, and the leaf balance pressure was measured with pressure chamber (model 1505D; PMS Instruments Co) and the balance pressure equated to T_{nx}. Soon after excising the leaves, *PLC* due to embolism was measured with the LPFM technique (measured on six 2-cm-long stem segments harvested under water from each shoot) as described before. Traditionally, stems are not flushed when VCs are measured by the bench top dehydration method; hence, native *PLC* was factored out of the bench top dehydration VCs using Eqn 5:

$$AdjPLC(T) = [PLC(T) - NPLC] = \frac{100}{(100 - NPLC)} \quad (5)$$

where $AdjPLC(T)$ is the adjusted *PLC* at xylem tension (T) and $PLC(T)$ is the *PLC* measured by the bench top method at any given T before correction for *NPLC*. Equation 5 basically re-scales the uncorrected VC by a constant factor of $[100/(100 - NPLC)]$, which starts at the *NPLC* at low tension and increases to $PLC(T) = 100\%$ at maximum tension.

VCs by air injection using a pressure collar

A pressure collar (model 1505D-EXP; PMS, Albany, OR, USA) was used to measure VCs according to Cochard *et al*. (1992) and Ennajeh *et al*. (2011). Briefly, stem segments of 15 or 27.4 cm long were harvested as above and flushed to achieve maximum hydraulic conductivity; the bark was removed from the central portion of the segment equal to the length of the pressure collar (8 cm), and mounted on the collar. The segment, while mounted on the collar, was connected to a LPFM for the measurement of K_{max}, as described earlier, and then removed from the LPFM and immersed in water while still connected to the collar. Segments were exposed to each test pressure for 10 min. At all times, the segment ends were immersed in water to observe bubbling of air that resulted from embolism under positive pressure. After the 10 min exposure, the pressure was returned to atmospheric and we waited until the bubbles had stopped flowing out of the ends (for 30 min or more) and then the K_h of the stem segment was measured in the LPFM. *PLC* was calculated from Eqn 2.

Measured and predicted *NPLC*

NPLC measurements were conducted in August on sunny days with maximum temperature above 31°C. Shoots were sampled in the afternoon between 1400 and 1500 h. Leaf balance pressure = the native xylem tension (T_{nx}) was measured by the pressure chamber method prior to excising shoots. *NPLC* was computed from K_h measured on 27.4-cm-long segments by two techniques: the LPFM technique and the Cavitron technique. In the Cavitron technique, the centrifuge was used to measure K_i and K_{max} before and after flushing at 500 r.p.m. ($T = 0.022$ MPa at the centre). The K_h values were also measured by the LPFM technique. The difference between techniques is the tension. K_h was measured at either positive pressure or a small sub-atmospheric pressure. The process for LPFM test was similar to the pre-dawn *PLC* test, with the difference that 27.4 cm stems were used. K_i and K_{max} measurements were made at 500 r.p.m. (tension = 0.022 MPa) after spinning for 40 min. Predicted *NPLC* was calculated from VCs measured on flushed samples in the Cavitron using the native tension T_{nx} measured in the field at the time of collection.

Stomatal conductance

Stomatal conductance (g_s) was measured using a Li-6400XT portable photosynthesis system (Li-Cor Inc., Lincoln, NE, USA) in a sunny day in August. Ten leaves from the four sample trees were tagged and measured from 0700 to 2000 h at 1 h intervals. Leaves were measured with natural sunlight, air temperature and ambient CO_2 while keeping the leaves in their native growing position during the measurement.

Anatomical observations and staining

Stem segments were stained to determine the diameter of conducting (stained) and embolized (unstained) vessels by a technique, as described in Cai *et al*. (2014). Shoots (>1.4 m in length) were collected in the afternoon between 1400 and 1500 h. Four stem segments 2 cm long and 6.5 mm in diameter were excised under water. Then, the segments were perfused with 0.02% (w/v) dying solution (basic fuchsin + 0.1 M KCl) at a pressure of 3 kPa. Four segments were perfused for 15 min, 30 min, 1 h and 2 h, respectively. Then, segments were flushed with 0.1 M KCl at 130 kPa for 5 min to remove excess stain. A microtome (Leica RM 2235, Nussloch, Germany) was used to cut 18-μm-thick cross sections from the middle of the 2 cm segments. Four sections were washed in graded ethanol (35, 50, 75 and 95%) for ≥4 s and mounted in glycerin on glass slides. Cross sections were photographed under a microscope (Zeiss, Imager A2, Göttingen, Germany) at 100× magnification with a digital camera (Infinity1-5C, Lumenera Corporation Ottawa, Canada). The RGB colour values, exposure, gamma and colour saturation were adjusted to yield suitable image quality using the software called Infinity Capture Application (Version 6.0.0, Lumenera Corporation Ottawa, Canada). Stained and unstained vessel areas (A) were measured with

WinCell Pro version 2012a (Regent Instruments Inc., Quebec City, Canada) and equivalent diameters (D) were computed from $D = 2(A/\pi)^{1/2}$.

RESULTS

Diameter and length of vessels

The frequency distribution of vessel diameter – percentage of vessels versus bin diameter size class (D) – is shown in Fig. 1a together with the hydraulic weight of the size classes. The hydraulic weight of each size classes is defined as % vessels $\times D^4$ in each diameter size class. The fourth power is used to weigh the hydraulic conductivity of each bin size class according to the Hagen–Poiseuille law. It can be seen that large-diameter vessels have a disproportionate hydraulic weight relative to the percentage of each bin diameter size class. Staining was used to determine which vessels were embolized (unstained) in the native state; the number of embolized vessels was 269 compared to the total vessels measured, 1239 (stained and unstained). In terms of hydraulic weight, the embolized vessels tended to be a little smaller, where the mode diameter of embolized vessels was about 60 μm versus 75 μm for all vessels.

We chose to measure vessel length by the air injection technique (Cohen *et al*. 2003) because it also averages (weighs) the vessel length towards the more conductive conduits. In the air injection technique, one can plot $\ln(C/C_0)$ versus distance from the air injection surface, where C is the pneumatic conductivity of the stem at distance x and C_0 is C at $x = 0$. The use of C for pneumatic flow is similar to water flow, which, like the Hagen–Poisseuille law, weighs air flow by the fourth power of the diameter of the conduit through which the air flows. According to Cohen *et al*. (2003), the slope of $\ln(C/C_0)$ versus distance x from the injection surface can be used to calculate vessel length. Three representative plots out of 12 experiments in which air was injected from the apical or basal end of six stems each are shown in Fig. 1b. Other advantages of the air injection technique are that it is faster than other standard techniques (Cai *et al*. 2010) and has a high R^2 (≥0.99) for the regression of the plot of $\ln(C/C_0)$ versus x used to determine mean vessel length. A final advantage of normalizing the plot of C to C_0, that is, $\ln(C/C_0)$, is that the anti-log directly yields the fraction of vessels still open at any given distance x from the injection surface (see right axis values in % in Fig. 1b).

There was no significant difference between vessel length computed whether air was injected from the apex or base of stems, so the values were pooled to yield a mean vessel length of 20 ± 1.9 cm ($n = 12$); all errors in this article are standard errors of the mean, unless otherwise stated. However, there was a large variation in the mean vessel length between stems between a maximum and minimum of 30.0 and 12.7 cm, respectively. The length of stem segments used in our Cavitron is 27.4 cm, the mean vessel length and percentage of vessels still open at the length and half-length of these segments are given in Table 1 for each segment as well as the overall means.

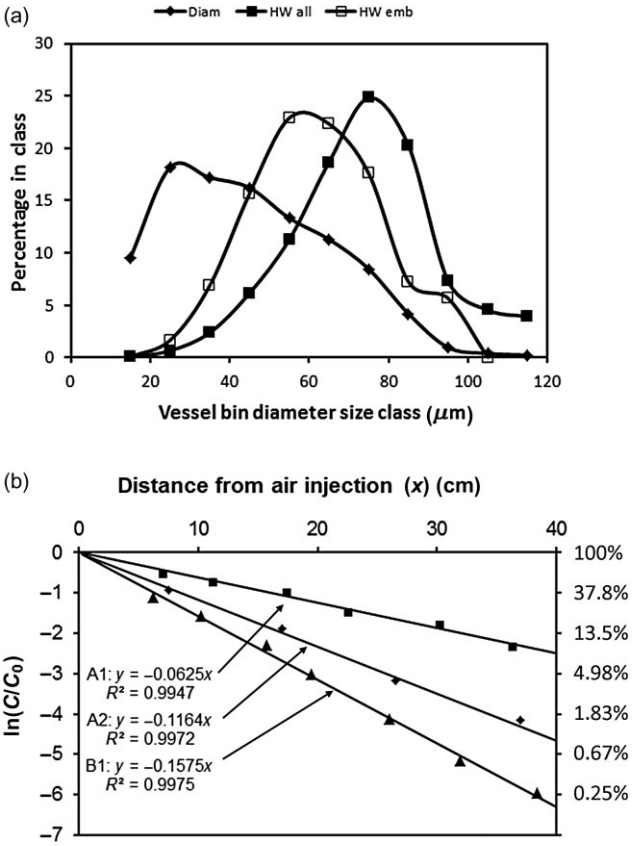

Figure 1. (a) Frequency distribution of vessel diameters plotted as percentage of vessels (y-axis) in each bin diameter size class (x-axis). Diamond points are a plot of the percentage of vessels in each diameter size class on the x-axis. The hydraulic weight (% in each class) is defined as $y_i D_i^4 / \sum(y_i D_i^4)$, where y_i is the percentage value on the y-axis of the diamond points and D_i is the diameter size class on the x-axis for the diamond points. The solid squares are the hydraulic weight of all vessels ($n = 1239$ vessels) and open squares are the hydraulic weight of embolized vessels in the native state ($n = 269$ vessels). (b) Three examples of air injection data for the determination of vessel length. Each data set contains at least 7 points, but some points used in the regression are beyond the maximum value of x (distance from the air injection surface). The y-axis is the natural log of C [pneumatic conductivity divided by C_0 (the limiting value of C as x approaches zero)]; C_0 is derived from the y-intercept of the regression of $\ln(C)$ versus x. The advantage of normalizing the plot to C_0 is that the anti-log (shown on the left axis) equals the fraction of vessels still open at distance x; the anti-log is given as a percentage on the right-hand vertical axis. A1 and A2 are branches injected from the apex and B1 was injected from the base. The slopes of the regressions are given in the figure and mean vessel length = –2/slope.

VCs measured by three methods

The VCs of *Robinia* measured by the Cavitron technique exhibited 'R'-shaped curves (Fig. 1a). The curves were fitted by both single and dual Weibull fits (Eqn 3a and 3b); the dual Weibull function fitted significantly better than that fitted by a single Weibull function (Table 2). The *PLC* rose fast with the increase of tension (induced by centrifuge) from 0% at 0.022 MPa to about 78% at 0.599 MPa. The increase of *PLC*

Table 1 Shown are vessel lengths of $n = 12$ stems injected with air from the apex or base

Method	Vessel length (cm)	% > 27.4 cm long	% > 13.7 cm long	Longest vessel (cm)
Apex injection	17.2	4.1%	20.3%	61
Apex injection	32.0 (max)	18.0%	42.5%	59
Apex injection	19.2	5.8%	24.0%	57
Apex injection	16.8	3.8%	19.5%	54
Apex injection	15.9	3.2%	17.8%	56
Apex injection	27.9	14.1%	37.5%	58
Base injection	14.9	2.6%	16.0%	32
Base injection	29.0	15.1%	38.9%	53
Base injection	22.1	8.3%	28.9%	46
Base injection	12.7 (min)	1.3%	11.6%	44
Base injection	16.3	3.4%	18.5%	51
Base injection	16.1	3.3%	18.2%	42
Mean	20.0	6.9%	24.5%	
SD	6.3	5.7%	10.1%	
SE	1.9	1.7%	3.0%	

Maximum and minimum values are indicated in the table; however, in Fig. 4b, we report a mean vessel length of 5.2 cm in one stem segment. The longest vessel length has a resolution of 2 cm (=length of segments excised).

slowed down as the tension grew higher than 0.599 MPa and reached 95% at 2.947 MPa. The shapes of VCs were not dramatically changed regardless of whether there is flushing (Fig. 2a) or not (Fig. 2b) prior to the VC measurements, and the P_{50} values were not significantly different ($P = 0.941$), with the values of 0.319 and 0.323 MPa for flushed and unflushed stems, respectively.

The VC constructed by the bench top dehydration technique is shown in Fig. 2b, which displayed an S-shaped curves. The *PLC* stayed at low levels (<10%) until tension exceeded 2.9 MPa. *PLC* dramatically increased from 6.39 to 97.27% as xylem tension rose from 2.9 to 4.6 MPa. The P_{50} equalled 3.57 MPa for bench top dehydration, which was about 11 times the P_{50} value calculated from Cavitron VCs. The VCs obtained by the air injection technique were also of S-shaped but intermediate between the R-shaped Cavitron curves and the S-shaped curves obtained by bench top dehydration (see Table 2 for parameters and statistics). The question is which VC is correct? Some clues can be gained by examining the water relations of the species below.

Table 2 Shown are the parameters from the single and dual Weibull fits (WF) in Eqns 3a and 3b, respectively

	Dual WF			
	Mean	SD	SE	$P_{1/2}$
B_1	0.280	0.081	0.022	0.223
C_1	1.595	0.717	0.199	
B_2	1.695	1.037	0.288	1.261
C_2	1.240	0.731	0.203	
α	68.2	10.389	2.881	
RMS_{error}	2.393	0.854	0.237	
	Single WF			
	Mean	SD	SE	P_{50}
B	0.436	0.124	0.034	0.295
C	0.939	0.233	0.065	
RMS_{error}	5.516	1.027	0.285	

The RMS_{error} of the fits are significantly different ($P < 10^{-8}$), $n = 14$.

Diurnal water relations and native *PLC* of *Robinia*

The diurnal variation of the water relations of *Robinia* on 3 sunny days in August is shown in Fig. 3a. The balance pressure of transpiring leaves provides an undefined estimate of minus leaf water potential ($P_{b,leaf} \cong -\Psi_{leaf}$). The estimate is undefined because a transpiring leaf has a water potential gradient that disappears when the leaf is enclosed in a pressure chamber; after the leaf is equilibrated in the pressure chamber, the balance pressure equals the xylem tension, which, in turn, equals the water potential minus the xylem osmotic pressure. The balance pressure of bagged leaves is traditionally taken as a measure of the native tension of stem xylem fluid (T_{nx}). From Fig. 3a, we can conclude that stems and leaves rehydrate to a balance pressure <0.3 MPa overnight and rise to approximately 1.6 and 1.8 MPa by midday, respectively. In contrast, stomatal conductance (g_s) peaks at 0800 h when stem and leaf balance pressures are about 0.8 and 1.1 MPa, respectively. Partial or complete *stomatal* closure is often viewed as a mechanism to avoid excessive embolism in stems, and in most cases, the minimum g_s occurs quite near the inflection point of the VC of the species in question, that is, when $PLC \leq 10\%$ (Cochard *et al.* 1996). In this context, the stomatal behaviour seems to fit superficially best with the air injection VC, which reaches 10% *PLC* at about 1 MPa (Fig. 2b). However, it could fit with the bench top dehydration VC if we argue that *Robinia* is very conservative in its water relations (see the Discussion section for more details). On the contrary, *Robinia* has been described as

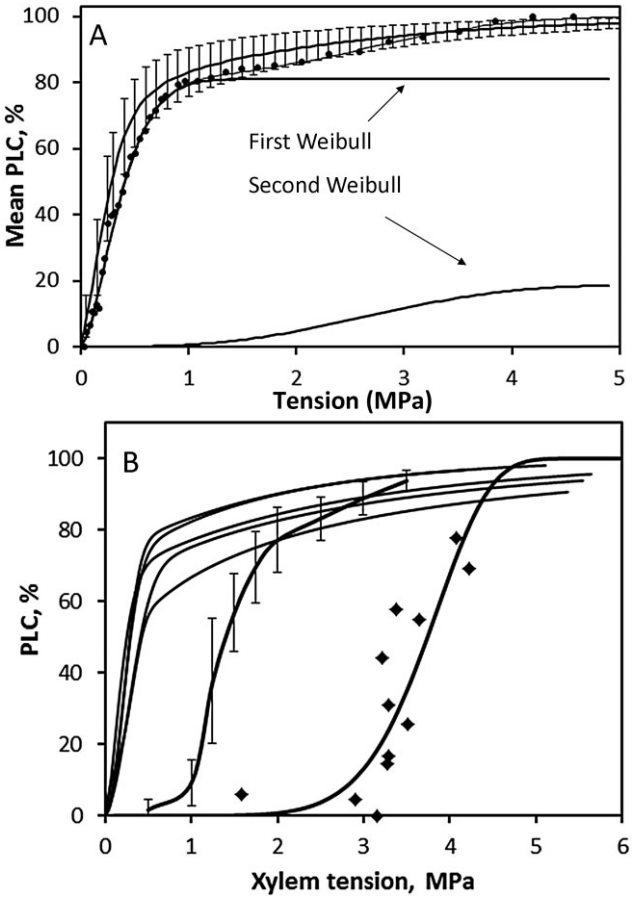

Figure 2. Vulnerability curves measured by three techniques. (a) The mean of 14 vulnerability curves (VCs) measured on flushed stems by the Cavitron technique. Each curve was fitted with a dual Weibull, then the mean and SD of all 14 best-fit curves were computed. The curve with dots is an example of a dual Weibull fit of one stem; the dual Weibull fit is the sum of two Weibulls as shown by arrows where the first is R-shaped and the second is S-shaped. (b) VCs measured by three techniques are shown. The five R-shaped curves were determined by the Cavitron technique on unflushed stem segments (mean $P_{50} = 0.323$ SE ± 0.032), the S-shaped curve with error bars is the mean and SE of 6 stems measured by air injection on flushed samples. The S-shaped curve with diamonds was determined by bench top dehydration on unflushed samples, with native state embolism correctons as in Eqn (5).

a species capable of refilling embolisms every night (An *et al.* 2006), and if it does refill nightly, then even the R-shaped VC might be accepted.

We reject the notion that the R-shaped curve is correct because of our observations of native *PLC* (Fig. 3b). The native *PLC* seems constant from May through August, with no significant change between pre-dawn and midday. Furthermore, if the R-shaped VCs were correct, then the midday T_{nx} (Fig. 3a) combined with the Cavitron VC (Fig. 2a) would predict a midday native *PLC* of about 85%, which is significantly different from the observed native *PLC* (around 30%) ($P < 10^{-10}$). Native *PLC*s in August were measured on Cavitron-sized stem segments (27.4 cm), and values of K_i and K_{max} were measured both in the Cavitron and in the LPFM. There was no significant difference in K_i, K_{max} or *PLC* measured by the LPFM or Cavitron (data not shown).

Time dependence of K_h measured inside the Cavitron

There is still a lot of debate and uncertainty about whether the Cavitron specifically or any centrifuge techniques in general can correctly measure VC on stem segments having vessels longer than half-length of the stems spinning in the centrifuge. While no one can prove the cause, most writers speculate that embolisms can be triggered by hydrophobic particles or tiny air bubbles pulled into stem segments while stems are spinning and these particles seed embolism (see the Discussion section); we might call this the 'particle seeding embolism' hypothesis or PSE hypothesis for short. If the PSE hypothesis is correct, we reasoned that if some PSE seed embolism at the top of the R-shape VC curve ($T = 1$ MPa in Fig. 2a), then other more 'vulnerable' particles have to be posited to cause seeding at the beginning of the VC curve (say

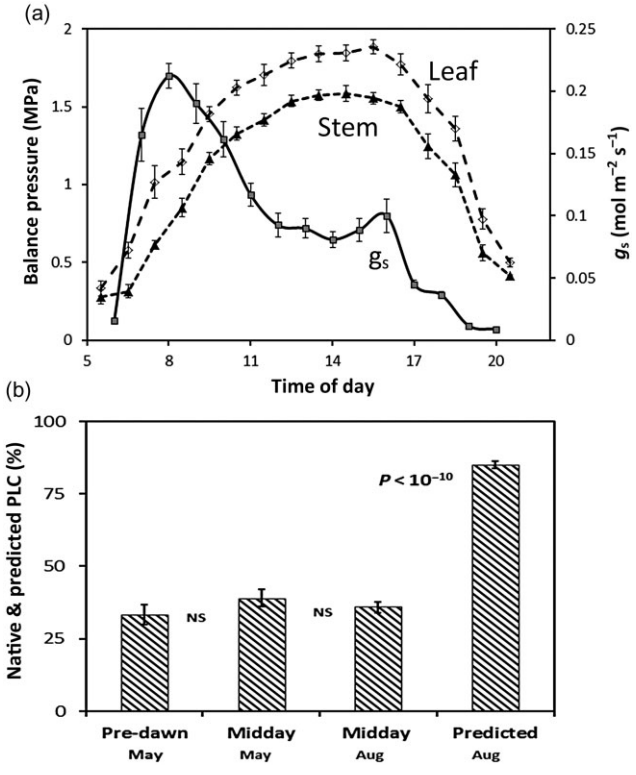

Figure 3. Diurnal water relations of *Robinia*. (a) Stomatal conductance (g_s), balance pressure of transpiring leaves and stem xylem tension on 3 days in August. Balance pressure can be equated to xylem tension. Shown are means and SE error bars ($n = 6$–10 for leaf and stem values and $n = 10$ for g_s values). (b) Measured and predicted native *PLC*. Native *PLC* was measured pre-dawn and midday in May and midday in August. The May measures of *PLC* were based upon $n = 32$ samples. The August *PLC*s were based upon $n = 12$ samples. The predicted value was based upon measured stem tensions (Fig. 3a) in August and the Cavitron VCs (Fig. 2a) (see text for details).

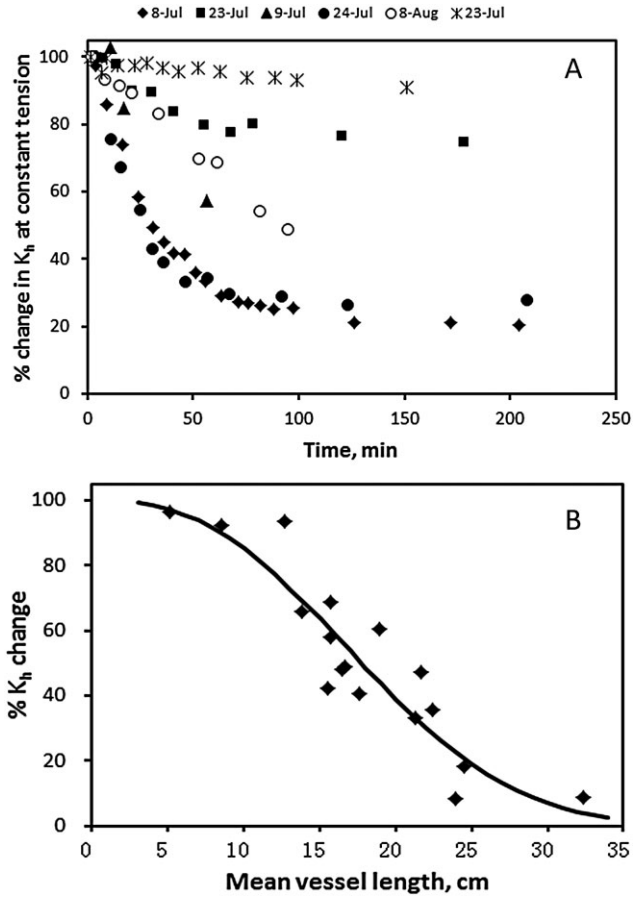

Figure 4. (a) This plot gives examples of the tempo of decline in K_h when tension is held constant. The *y*-axis is the percentage of the initial K_h near time zero (Cavitron spinning at 500 r.p.m. = tension of 0.031 MPa). We estimate that during these experiments the total volume of water passing through the stems was <1.1 cm^3 in stems 27.4 cm long with a total wood volume of 16 cm^3. (b) The *y*-axis is the percentage initial K_h after 4 h of measurements at 900 r.p.m. = tension of 0.072 MPa. The *x*-axis is the mean vessel length measured by the air injection method on the same stem segment.

at $T = 0.1$ MPa in Fig. 2a). However, if the highly vulnerable particles are posited that seed at 0.1 MPa, then these particles must always be present. Hence, we predicted that extensive embolism should happen if we just spin stem segments with long vessels for long enough time for the most vulnerable particles to be passed through most of the vessels. The experiment testing the PSE hypothesis is shown in Fig. 4a. In this experiment, stem segments were held at a constant tension of 0.031 MPa (500 r.p.m.) for nearly 4 h. Each point in Fig. 4a represents the mean of two to seven K_h measurements made in the Cavitron at each time shown on the *x*-axis. The results have been scaled to give K_h as a percentage of the first (initial) value of K_h measured near time zero.

Figure 4b further explores the PSE hypothesis by correlating the percentage of the initial K_h observed after 4 h of spinning and repeated measurements of K_h at 900 r.p.m. ($T_x = 0.072$ MPa) versus the mean vessel length observed in the segment. This experiment was possible because of the high variability in mean vessel length between *Robinia* segments. It can be seen that the percentage of the initial K_h is a sigmoid function of the mean vessel length. These results are consistent with the PSE hypothesis and are consistent with the existence of very vulnerable particles that cause embolism at low tension.

DISCUSSION

Our experiments revealed three quite different VCs obtained by the three techniques. One curve is R-shaped and the other two are S-shaped with P_{50} values of about 0.6, 1.5 and 3.6 MPa. Only one of the VCs reported in this article is likely to be true. So we must examine the veracity of each curve below.

The R-shaped curve measured by the Cavitron (Fig. 2a) had a P_{50} inconsistent with the diurnal water relations of the species (Fig. 3a) because the midday xylem tensions, combined with the R-Shaped curve, predicted a native *PLC* significantly higher than observed (Fig. 3b) (about 85% versus 30%). There is also no evidence for a daily cycle of embolism formation and embolism repair because *NPLC* did not change from midday to pre-dawn. This is in contrast to oak species studied by Sperry, which seemed to embolize every day and refill nightly (Taneda & Sperry 2008); however, it is not clear to us if Sperry now thinks differently about his specific experiment (see Sperry 2013; Wheeler *et al.* 2013).

The S-shaped curve obtained by the air injection method superficially seems to fit best with the water relations and native embolism because the VC, combined with the daily water relations, predicts a *NPLC* close to that observed but we tentatively reject the notion because there is a known vessel length artefact associated with the air injection method (Ennajeh *et al.* 2011). In contrast, the S-shaped curve from the bench top dehydration method seems to predict *NPLC* values <5%. However, the bench top dehydration curve was measured on unflushed stems, so the native embolism was factored out of the curve plotted in Fig. 3b. Ennajeh *et al.* (2011) noted a vessel length error in the air injection method, causing an underestimate of P_{50} when vessels are longer than the injection chamber. Hence, on the basis of the above observations, we accept the bench top dehydration curve over the air injection curve. The bench top dehydration curve also fits best with the stomatal conductance data and the notion of 'the conservative plant' (see below).

Both Sperry *et al.* (2012) and Cochard *et al.* (2013) suggested that the Cochard technique overestimates the vulnerability of vessels in species with vessels that are predominately at least half as long as the segment spinning in the Cavitron. In a recent review, Cochard *et al.* (2013) refers to R-shaped curves as 'exponential' and concludes a valuable meta-analysis of VC data from hundreds of species with the statement that, 'It is important to realize that beyond the "exponential" versus "sigmoidal" shape debate it is the physiology and the ecological significances of cavitation that is involved.' He goes on to explain that S-shaped curves fit with a physiology in which stomata close at xylem tensions prior

to the onset of much embolism in stems (Crombie *et al*. 1985; Jones & Sutherland 1991). In the 'sigmoidal' paradigm, drought tolerance is genetically determined by whatever controls the P_{50} of the sigmoidal curve. In contrast with the R-shaped physiological paradigm, cavitation forms under very mild water stress. As a corollary, embolized vessels must refill at night for the plant to survive or the plant must function with most vessels permanently embolized. Drought tolerance in these species may be linked to the ability of the plant to refill. Cochard's meta-analysis reveals that the Sperry centrifuge technique measures R-shaped curves in 85% of the species with long vessels, whereas the bench top dehydration method measures R-shaped curves in only 15% of the species with long vessels, whereas both techniques yield S-shaped curves in most short-vessel species. The physiology of *Robinia* is consistent with the S-shaped physiology. For the first time, our study provides further clues regarding why the Cochard technique might yield wrong VCs.

Of bubbles and particles

Figure 4 provides some interesting clues about what might be causing the R-shaped curves in *Robinia*. Both Cochard *et al*. (2010) and Sperry *et al*. (2012) suggested that loss of K_h might be caused by foreign bodies (solid particles or small air bubbles) passing through the cut-open vessels in the Cochard Cavitron. We will describe 'particulate' water as water-containing solid nanometre-sized particles and 'effervescent' water as water-containing bubbles. The behaviour of particulate and effervescent water could be quite different because bubbles could seed a cavitation at tensions less than that of a perfect vacuum (<0.1 MPa), but particles might resist cavitation to higher tensions. If the vessels are short enough, the vessel ends will filter out the foreign bodies before they migrate further towards the centre of the spinning stem segment where tensions are low enough for the particles to seed cavitation or block vessels. Figure 4a, however, provides quite new insights because in this experiment the induced loss of K_h is not a function of tension but instead seems to depend upon the *time* taken to repeatedly measure K_h, while tension is held constant <0.1 MPa. So we have to entertain the notion that the R-shaped curve of some species might be caused by the time it takes to measure the VC and not by the value of tension on the *x*-axis of a VC.

The parsimonious explanation is that the loss of K_h in Fig. 4a is caused by particles blocking the flow when the particles are caught up by pit membranes in closed vessels; hence, everything could be explained by particulate water. We reject the parsimonious explanation because we could suppose that the water contains nanoparticles on some days but not on others. In parallel experiments, a PhD student in our laboratory was using the same ultra-filtered water on the same days to flush a *Populus* clone with short vessels 6 cm long (Feng Feng, personal communication). Feng used the Cavitron to measure VCs and induced >96% *PLC* on flushed stems. Feng then re-flush the stems for 30 min and could restore the original maximum K_h after measuring the VC of *Populus* stems. If the water had been particulate, then flushing would have resulted in a lower K_{max}, and indeed before our laboratory started using an ultra-filtration system and before cleaning the water tanks frequently, we were unable to flush embolized stems back to the initial K_{max}. Finally, if the water had been filled with nanoparticles, then the 'plugging' of vessels should have been more in stems with short vessels than long vessels, but the opposite seems to be true in Fig. 4b.

Could bubbles explain the behaviour in Fig. 4?

We found that the vessel length of *Robinia* stems is quite variable between segments, with mean vessel length ranging from 5 to 33 cm. The sigmoid curve in Fig. 4b is a Weibull fit with an RMS_{error} of 10.4%, and it appears that the percentage initial K_h (after 4 h of measurements) decreases with increasing vessel length. This suggests that the loss of K_h is caused by effervescent water, that is, by air bubbles rather than nanoparticles. Sperry *et al*. (2012) suggested that air bubbles might be created at the moment water is injected into the basal reservoir of the Cochard Cavitron, which is made out of a spectrometer cuvette (see fig. 1 in Sperry *et al*. 2012). The air bubbles might be created by the velocity with which the stream of water strikes the surface of water in the reservoir. This phenomenon of bubble creation can be recreated in a cuvette by directing a stream of water from a hypodermic needle onto the surface of water by pushing on the plunger of the syringe attached to the needle. While we cannot prove that the bubbles are generated inside our Cavitron during injection while the stem is spinning, we can speculate about the size of the air bubbles needed to seed 'cavitation' at the low angular velocity (r.p.m.) used in the experiments in Fig. 4.

Tiny air bubbles are inherently unstable because of the surface tension of water. They expand or contract depending upon the pressure of the air bubble, which depends upon the surface tension of the air–water interface and the pressure of the water surrounding the bubble. Expansion could be very fast when the pressure of the water is low enough to cause a vacuum void in the bubble. However, according to Henry's law of gas solubility in water, expansion can happen whenever the gas pressure in the bubble is less than the atmospheric pressure because air will come out of the solution to fill the bubble with more air. Expansion happens when the water pressure is below a certain critical value and collapse happens (by bubble dissolution into water) when the pressure is above the critical pressure (P_{crit}). There is only one pressure at which a bubble is stable and that pressure depends upon the bubble radius (r). Hence, in a Cavitron, most bubbles will tend to collapse in the cuvette because the water pressure is positive due to the centrifugal force acting on the water column in the cuvette. How long it takes bubbles to expand or collapse is beyond the scope of this article, but readers may refer to Yang & Tyree (1992), Tyree & Yang (1992), and Wang *et al*. (2013) for some insights into timing. Suffice it to say that if bubbles enter cut-open vessels and start migrating towards the axis of rotation, they will tend to grow smaller until they reach the position in the segment where the water pressure is below the critical pressure that

causes them to expand again. The details of this process of bubble expansion in the context of a Cavitron have never been discussed in the literature so this concept is developed below.

The critical pressure for bubble stability happens when the air pressure in the bubble equals the atmospheric pressure, assuming the water is saturated with air at atmospheric pressure because, according to Henry's law, the saturation concentration of gases in water depends upon the partial pressure of the gas in contact with the air. At the altitude of our laboratory (450 m), the standard atmospheric pressure is 100 kPa; hence, if the bubble pressure is >100 kPa, air will dissolve in water and the bubble will collapse, and if the bubble pressure is <100 kPa, it will expand. The expansion will require enough time for the movement of gas molecules from the liquid phase to the gaseous phase in the air bubble (Henry's law), which will increase r until it equals the vessel radius; since this process will require time, the bubble will have to be trapped in the vessel long enough for the expansion process to finish. The critical pressure can be computed from the surface tension of water (τ) surrounding an air bubble of radius (r):

$$\frac{2\tau}{r} = (P_b - P_W) \tag{6a}$$

where P_b is the air pressure in the bubble and P_w is the water pressure. P_{crit} is defined as the P_w value that makes P_b = atmospheric pressure (typically 100 kPa depending upon the barometric pressure): $P_{crit} = 100 - 2\tau/r$. In Cavitron experiments, we define tension (T) as the difference between barometric pressure and water pressure so the critical T (T_{crit}) = 100 – P_{crit}; hence,

$$T_{crit} = \frac{2\tau}{r} \tag{6b}$$

Figure 5 shows a plot of T_{crit} versus r. The open circles represent the T values used in Fig. 4. In Fig. 4a, the RPM was 500, corresponding to T = 32 kPa, and in Fig. 4b, the RPM was 900, corresponding to T = 72 kPa. From the critical tension curve, we can conclude that the bubbles needed to be bigger than 4.5 μm (T = 32 kPa) and 2.0 μm (T = 72 kPa) to expand and cause a decline in K_h as the bubbles passed through the centre of the stem segments. From Fig. 1a (squares), it can be seen that the (most common) vessel radius that accounts for K_h is around 35 μm (70 μm diameter on the x-axis); hence, bubbles as large as predicted in Fig. 5 could easily pass through the vessels of *Robinia* because vessel elements have simple perforation plates capable of passing air bubbles >5 μm (Sherwin Carlquist, personal communication) and this is confirmed using a maceration technique.

More work needs to be done to confirm the suggestions advanced in the previous paragraph, that is, that bubbles cause the time-dependent embolism in Fig. 4 at constant tension. However, the results in Fig. 4 stand even if the effervescent water hypothesis turns out to be wrong.

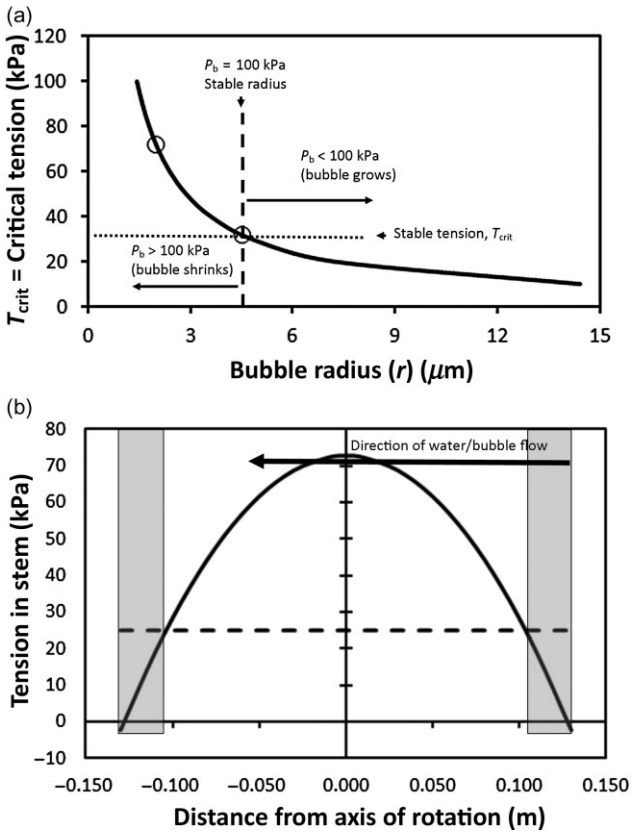

Figure 5. (a) Shown is a plot of Eqn 6b. The y-axis is the critical tension for bubble stability versus bubble radius on the x-axis. When a bubble experiences water at a tension more than T_{crit}, it should expand to seed a cavitation and the consequent loss of K_h, and when the water tension is <T_{crit}, it should slowly collapse as the air dissolves in the surrounding water. (b) This diagram shows the regions of instability for a bubble as it passes through a stem segment in a Cavitron spinning with a central tension of 72 kPa. The bell-shaped curve is a plot of tension versus distance from the axis of rotation. A bubble of 9 μm radius will have a critical tension of 25 kPa. In the grey areas, the bubble will shrink, and in the clear areas, it will expand. The bubble is stable only at the interface between the grey and clear areas.

Stomatal regulation and the conservative plant

The notion has been advanced several times (see, e.g. Tyree & Sperry 1988; Jones & Sutherland 1991; Cochard *et al*. 1996; Arango-Velez *et al*. 2011) that stomatal regulation in plants has evolved to avoid cavitation in any given species. According to the soil plant continuum model, we can postulate that tension in the xylem (T_x) will depend upon soil water potential (Ψ_{soi}), the water flow rate through the pathway from the soil to the leaf-bearing stems (F_x) and the resistance to water flow from soil to stems (R_x); hence,

$$T_x = R_x F_x - \Psi_{soil} = R_x A g_l \Delta X - \Psi_{soil} \tag{7}$$

In Eqn 7, we have substituted for $F_x = Ag_l\Delta X$, where A is the leaf area attached to the stem, g_l is the leaf conductance to water vapour = stomatal + cuticular conductance, and ΔX

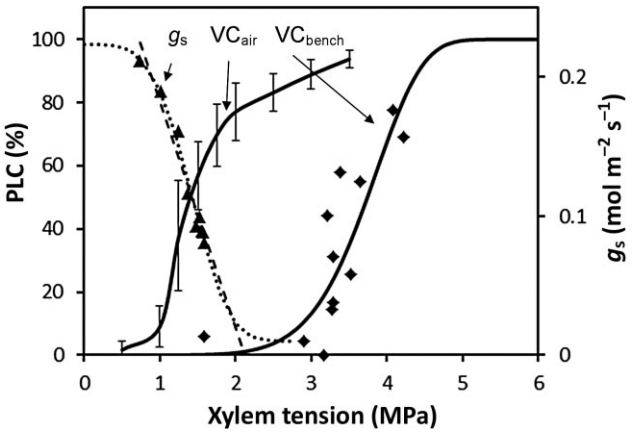

Figure 6. The stomatal conductance (g_s) (triangles) in Fig. 3a was re-plotted as a function of xylem tension (T_x), together with the vulnerability curve obtained by air injection (VC_{air}) and the vulnerability curve obtained by bench top dehydration. See text for details of the criteria for selection of g_s values. The straight dashed line is a simple linear regression of g_s versus T_x. The leaf transpiration is a sum cuticular and stomatal conductance to water vapour. The sigmoid-dashed line was plotted to indicate how whole leaf conductance might change over the same range of T_x, assuming cuticular conductance was 5% of leaf conductance.

is the driving force on evaporation (change in mole fraction of water vapour between the leaf and air). Hence, Eqn 7 shows the theoretical functional dependence of T_x on g_l ($\cong g_s$). Stomatal conductance will depend upon light, CO_2 concentration and water stress directly or chemical signalling driven by water stress. Figure 6 shows how g_s depends upon T_x (a measure of water stress) when light intensity is likely to be high enough to stimulate opening and CO_2 concentration are likely to be relatively constant, that is, from about 0900 to 1600 h in Fig. 3a. We plot this relationship together with the two S-shaped VCs.

It can be seen from Fig. 6 that the air injection VC does not follow the model of a conservative plant because g_l (dotted line) does not drop to a minimum value soon enough. We also tentatively reject the air injection VC because Ennajeh *et al.* (2011) has reported an 'open vessel' effect when the pressure collar used to measure VCs by air injection is shorter than the vessel length, that is, P_{50} is underestimated. In our case, the PMS pressure collar is 8 cm long versus the average vessel length of 20 cm. Until we can custom fabricate longer pressure collars, we have to tentatively accept the bench top dehydration curve, which is sometimes considered to be the 'gold standard' technique for determining VCs (Cochard *et al.* 2013).

CONCLUSIONS

The R-shaped curves are invalid because they do not fit with the water relations of *Robinia* (Fig. 3), because the R-shaped curve predicted a very high midday *NPLC* not observed in our data. The preponderance of evidence presented in this article supports the notion that the air bubbles cause premature embolism in the Cavitron (effervescent water hypothesis). Air bubbles appear to cause embolism in stems with long vessels but not short vessels (Fig. 4b). The amount of embolism increased with time then stabilized with repeated measurement of K_h while tension is held constant. Hence, R-shaped curves are probably a function of both time and tension. In contrast, the S-shaped VCs measured by the bench top dehydration method and the air injection method are in better agreement with the water relations of *Robinia*. The bench top dehydration curve seems more realistic than the air injection curve because it fits best with stomatal regulation (Fig. 6) and the notion of a conservative plant that closes stomata to avoid embolism. It seems very important that someone with access to a Sperry-type centrifuge perform the experiment in Fig. 4 to see if repeated measures of K_h result in a decline of conductivity. In a Sperry centrifuge technique, bubbles might be drawn into vessels while starting the spin or while mounting or dismounting the stems in the conductivity apparatus or both.

ACKNOWLEDGMENTS

The authors wish to acknowledge the following grants that made this research possible: Natural Science Foundation of China (Grant No. 31270646) to J.C. and the 'thousand talent program' grants to M.T.T.

REFERENCES

An F., Cai J., Jiang Z., Zhang Y., Lan G. & Zhang S. (2006) Refilling of embolism in the xylem of eight tree species and its relationship with pressure-volume parameters. *Journal of Northwest A & F University (Natural Science Edition)* **34,** 38–44.

Arango-Velez A., Zwiazek J.J., Thomas B.R. & Tyree M.T. (2011) Stomatal factors and vulnerability of stem xylem to cavitation in poplars. *Physiologia Plantarum* **143,** 154–165.

Brodersen C.R., McElrone A.J., Choat B., Matthews M.A. & Shackel K.A. (2010) The dynamics of embolism repair in xylem: *in vivo* visualizations using high-resolution computed tomography. *Plant Physiology* **154,** 1088–1095.

Cai J. & Tyree M.T. (2010) The impact of vessel size on vulnerability curves: data and models for within-species variability in saplings of aspen, *Populus tremuloides* Michx. *Plant, Cell & Environment* **33,** 1059–1069.

Cai J., Zhang S. & Tyree M.T. (2010) A computational algorithm addressing how vessel length might depend on vessel diameter. *Plant, Cell & Environment* **33,** 1234–1238.

Cai J., Li S., Zhang H., Zhang S. & Tyree M.T. (2014) Recalcitrant vulnerability curves: methods of analysis and the concept of fibre bridges for enhanced cavitation resistance. *Plant, Cell & Environment* **37,** 35–44.

Cochard H. (2002) A technique for measuring xylem hydraulic conductance under high negative pressures. *Plant, Cell & Environment* **25,** 815–819.

Cochard H., Cruiziat P. & Tyree M.T. (1992) Use of positive pressures to establish vulnerability curves: further support for the air-seeding hypothesis and implications for pressure-volume analysis. *Plant Physiology* **100,** 205–209.

Cochard H., Breda N. & Granier A. (1996) Whole tree hydraulic conductance and water loss regulation in *Quercus* during drought: evidence for stomatal control of embolism? *Annales des Sciences Forestieres. Sciences* **53,** 197–206.

Cochard H., Damour G., Bodet C., Tharwat I., Poirier M. & Améglio T. (2005) Evaluation of a new centrifuge technique for rapid generation of xylem vulnerability curves. *Physiologia Plantarum* **124,** 410–418.

Cochard H., Herbette S., Barigah T., Badel E., Ennajeh M. & Vilagrosa A. (2010) Does sample length influence the shape of xylem embolism vulnerability curves? A test with the Cavitron spinning technique. *Plant, Cell & Environment* **33,** 1543–1552.

Cochard H., Badel E., Herbette S., Delzon S., Choat B. & Jansen S. (2013) Methods for measuring plant vulnerability to cavitation: a critical review. *Journal of Experimental Botany* **64,** 4779–4791.

Cohen S., Bennink J. & Tyree M.T. (2003) Air method measurements of apple vessel length distributions with improved apparatus and theory. *Journal of Experimental Botany* **54,** 1889–1897.

Crombie D., Milburn J. & Hipkins M. (1985) Maximum sustainable xylem sap tensions in Rhododendron and other species. *Planta* **163,** 27–33.

Ennajeh M., Nouiri M., Khemira H. & Cochard H. (2011) Improvement to the air-injection technique to estimate xylem vulnerability to cavitation. *Trees* **25,** 705–710.

Jones H. & Sutherland R. (1991) Stomatal control of xylem embolism. *Plant, Cell & Environment* **14,** 607–612.

Salleo S., Lo Gullo M.A., De Paoli D. & Zippo M. (1996) Xylem recovery from cavitation-induced embolism in young plants of *Laurus nobilis*: a possible mechanism. *New Phytologist* **132,** 47–56.

Sperry J. (2013) Cutting-edge research or cutting-edge artifact? An overdue control experiment complicates the xylem refilling story. *Plant, Cell & Environment* **36,** 1916–1918.

Sperry J., Donnelly J. & Tyree M. (1988) A method for measuring hydraulic conductivity and embolism in xylem. *Plant, Cell & Environment* **11,** 35–40.

Sperry J.S., Christman M.A., Torres-Ruiz J.M., Taneda H. & Smith D.D. (2012) Vulnerability curves by centrifugation: is there an open vessel artefact, and are 'r' shaped curves necessarily invalid? *Plant, Cell & Environment* **35,** 601–610.

Taneda H. & Sperry J.S. (2008) A case-study of water transport in co-occurring ring-versus diffuse-porous trees: contrasts in water-status, conducting capacity, cavitation and vessel refilling. *Tree Physiology* **28,** 1641–1651.

Tyree M.T. & Dixon M.A. (1986) Water stress induced cavitation and embolism in some woody plants. *Physiologia Plantarum* **66,** 397–405.

Tyree M.T. & Sperry J.S. (1988) Do woody plants operate near the point of catastrophic xylem dysfunction caused by dynamic water stress? Answers from a model. *Plant Physiology* **88,** 574–580.

Tyree M.T. & Yang S. (1992) Hydraulic conductivity recovery versus water pressure in xylem of *Acer saccharum*. *Plant Physiology* **100,** 669–676.

Tyree M.T. & Zimmermann M.H. (2002) *Xylem Structure and the Ascent of Sap*, 2nd edn, Springer-Verlag, Berlin.

Tyree M.T., Cochard H., Cruiziat P., Sinclair B. & Ameglio T. (1993) Drought-induced leaf shedding in walnut: evidence for vulnerability segmentation. *Plant, Cell & Environment* **16,** 879–882.

Wang M., Tyree M.T. & Wasylishen R.E. (2013) Magnetic resonance imaging of water ascent in embolized xylem vessels of grapevine stem segments. *Canadian Journal of Plant Science* **93,** 879–893.

Wheeler J.K., Huggett B.A., Tofte A.N., Rockwell F.E. & Holbrook N.M. (2013) Cutting xylem under tension or supersaturated with gas can generate PLC and the appearance of rapid recovery from embolism. *Plant, Cell & Environment* **36,** 1938–1949.

Yang S. & Tyree M.T. (1992) A theoretical model of hydraulic conductivity recovery from embolism with comparison to experimental data on *Acer saccharum*. *Plant, Cell & Environment* **15,** 633–643.

Zhang S. & Richter H. (1996) The refilling of embolized xylem in *Taxus baccata* L. *Journal of Northwest Forestry College* **11,** 5–8.

Zwieniecki M. & Holbrook N. (1998) Diurnal variation in xylem hydraulic conductivity in white ash (*Fraxinus americana* L.), red maple (*Acer rubrum* L.) and red spruce (*Picea rubens* Sarg.). *Plant, Cell & Environment* **21,** 1173–1180.

Received 4 January 2014; received in revised form 17 February 2014; accepted for publication 24 February 2014